ELSEVIER

Contents lists available at ScienceDirect

Materials Letters

journal homepage: www.elsevier.com/locate/matlet



Orientation dependence of indentation behavior in Al–SiC nanolaminate composites



C. Mayer ^a, L.W. Yang ^b, S.S. Singh ^a, H. Xie ^a, Y.-L. Shen ^c, J. Llorca ^{b,d}, J. Molina-Aldareguia ^b, N. Chawla ^{a,*}

- ^a Materials Science and Engineering Arizona State University, Tempe, AZ 85287, USA
- ^b IMDEA Materials Institute, c/ Eric Kandel 2, 28906 Getafe, Madrid, Spain
- ^c Department of Mechanical Engineering, University of New Mexico, Albuquerque, NM, USA
- d Department of Materials Science. Polytechnic University of Madrid. E. T. S. de Ingenieros de Caminos, 28040 Madrid, Spain

ARTICLE INFO

Article history: Received 20 October 2015 Accepted 10 January 2016 Available online 11 January 2016

Keywords:
Nanoindentation
Nanolaminate
Multilayer
Anisotropy
Finite element modeling

ABSTRACT

Al and SiC nanolaminate films were characterized in the perpendicular, inclined and parallel orientations using nanoindentation. The deformation was dominated by buckling of the layers when the layers were parallel to the indenter and by compression of the ductile Al layers when the layers were perpendicular to the indenter, while indentation in inclined orientations showed an intermediate behavior. Finite element modeling (FEM) of indentation deformation using wavy layers showed much more compliant behavior and prominent layer buckling than the idealized flat structure, highlighting the large effect these microstructural details can have on the deformation behavior.

© 2016 Elsevier B.V. All rights reserved.

1. Introduction

Nanolaminate materials are a relatively new and promising class of composites that exhibit exceptional mechanical properties [1–3] as well as possible applications in bioengineering [4] and optics [5]. Although there is a growing body of research investigating the mechanical properties in the direction normal to the layers, there is very little work examining the effect of layer orientation relative to the loading axis.

The thickness of these films is limited to the order of micrometers by the fabrication method and therefore the mechanical testing is restricted to small-scale techniques. The experimental aspects of this work utilize nanoindentation, which has been used to characterize the mechanical properties of many small scale materials, including previous work on the Al–SiC nanolaminate system [1,6–9].

Isostress and isostrain loading are the most classical conditions to understand the mechanical properties of composite materials because they provide bounds for the elastic behavior. For a given composite volume fraction, as a first approximation, the isostress condition is expected to have the lowest stiffness while the isostrain condition leads to the highest stiffness [10]. While the previous work on nanolaminates focuses on loading in the

E-mail address: nchawla@asu.edu (N. Chawla).

perpendicular orientation [1–3,11–13], which approximates isostress deformation, no studies have compared this to the deformation in other orientations.

Recent modeling studies by Jamison and Shen [14] have shown the effect of initial layer waviness on the plane strain deformation of these structures. Under idealized uniaxial loading conditions parallel to the layers their modeling showed a large drop in stiffness as layer curvature increased while perpendicular to the layers, the effect is smaller but not negligible. The effect of this waviness on the mechanical properties has not been largely overlooked, with the vast majority of previous modeling efforts assuming perfectly flat microstructures [1,15,16]. Additionally, Verma and Jaryam [17] showed that under indentation loading normal to the film, the layer curvature increases the tensile stresses that develop causing an increase in delamination. However, their work only looked at the specific case of thick ceramic layers (\sim 150 nm ZrN) paired with thin metallic layers (\sim 10 nm Zr), which do not show the buckling behavior observed in our work when the layers are able to co-deform.

This work expands on the current literature by determining the deformation behavior of metal-ceramic multilayers under loading over a range of orientations using finite element modeling (FEM) and comparing this behavior to what is observed experimentally using indentation in the parallel, inclined at 45° and perpendicular orientations. To our knowledge, this has not been investigated in any nanolaminate system previously. As the previous work by Jamison and Shen indicated that the mechanical properties of these

^{*} Corresponding author.

Table 1Hardness and modulus values determined using nanoindentation for different orientations as well as the calculated modulus values using classical laminate theory.

	Perpendicular	45° Inclined	Parallel
H _{ind} (GPa) E _{ind} (GPa) E _{calc} (GPa)	$4.8 \pm 0.4 \\ 111 \pm 8 \\ 97$	$6.1 \pm 0.2 \\ 114 \pm 3 \\ 100$	6.9 ± 0.3 126 ± 4 168

materials can be highly sensitive to the initial waviness, the FEM simulations in this work utilize both idealized flat microstructures and more realistic wavy microstructures.

2. Materials and methods

An automated physical vapor deposition system was used to fabricate Al–SiC nanolaminates on a Si substrate. These laminates consisted of films with an individual layer thicknesses of 50 nm, with an overall multilayer thickness of 15 μm . The details of this process have been discussed in previous work [18]. Indentations made in the perpendicular orientation were characterized without further sample preparation. For the parallel and inclined directions, a diced wafer section, approximately $5\times 5~mm^2$, was mounted in epoxy such that the film would be oriented 90° and 45° , respectively, from the epoxy surface. To expose the edge of the film for testing, the mounted sample was then ground using SiC paper, and final polishing was carried out using $0.05~\mu m$ colloidal silica.

Indentations were performed using a commercial nanoindenter (Nanoindenter XP, Agilent) equipped with a Berkovich geometry diamond tip (displacement controlled, 5 s hold time). The system was left to stabilize until the drift rate was less than 0.05 nm/s. The continuous stiffness measurement (CSM) technique was used in order to determine the modulus and hardness as a function of indentation depth by superimposing a small harmonic load [19].

Since the sample width was limited to the multilayer thickness in the parallel and inclined cases, indentation depths were limited to 500 nm in order to minimize the contribution from the adjacent Si wafer and mounting epoxy. To obtain accurate results from this shallow indentation depth, the dynamic contact module (DCM) head was used, allowing higher load and displacement resolution [20]. For direct comparison, the same 500 nm depth was used for indentations in the perpendicular direction as well. The modulus and hardness values were calculated in the depth range of 100–200 nm for all tests. About 15 indentations were conducted in each of the orientations. A dual beam SEM/FIB was used to cross-section the indentations to see the difference in deformation behavior in both directions and to compare to FEM results.

Two-dimensional (2D) multilayer models were constructed for the finite element analysis using the program ABAQUS (Version 6.12, Dassault Systemes Simulia Corp., Providence, RI). The model geometry assumes a width and height of 10 µm and 50 µm, respectively, containing explicit 50 nm-thick layers of Al and SiC and a total of 328,000 four-noded linear plane-strain elements. Indentation was simulated by pressing a rigid angular indenter, with a half-angle of 68°, onto the top face of the material. Ten multilayer scenarios were considered: both flat and wavy layers in orientations with 0 (parallel), 10°, 20°, 45°, and 90° (perpendicular) angles between the loading axis and the layer direction. The undulations in the wavy layers were modeled as a sinusoidal waveform with a wavelength of 0.5 µm and an amplitude of 15 nm. The bottom boundary was fixed in space, and the two lateral boundaries were unconstrained during deformation. The elastic-plastic properties of Al and SiC, obtained from experimental measurements, were identical to those used in our previous study [11]. The Young's moduli for Al and SiC were 59 GPa and 277 GPa, respectively, and the corresponding Poisson's ratios were 0.33 and 0.17, respectively. The yield strengths of Al and SiC were 200 MPa and 8770 MPa, respectively, with initial strain hardening for Al included leading to a constant flow stress of 400 MPa [11].

As the true indentation modulus is unable to be calculated

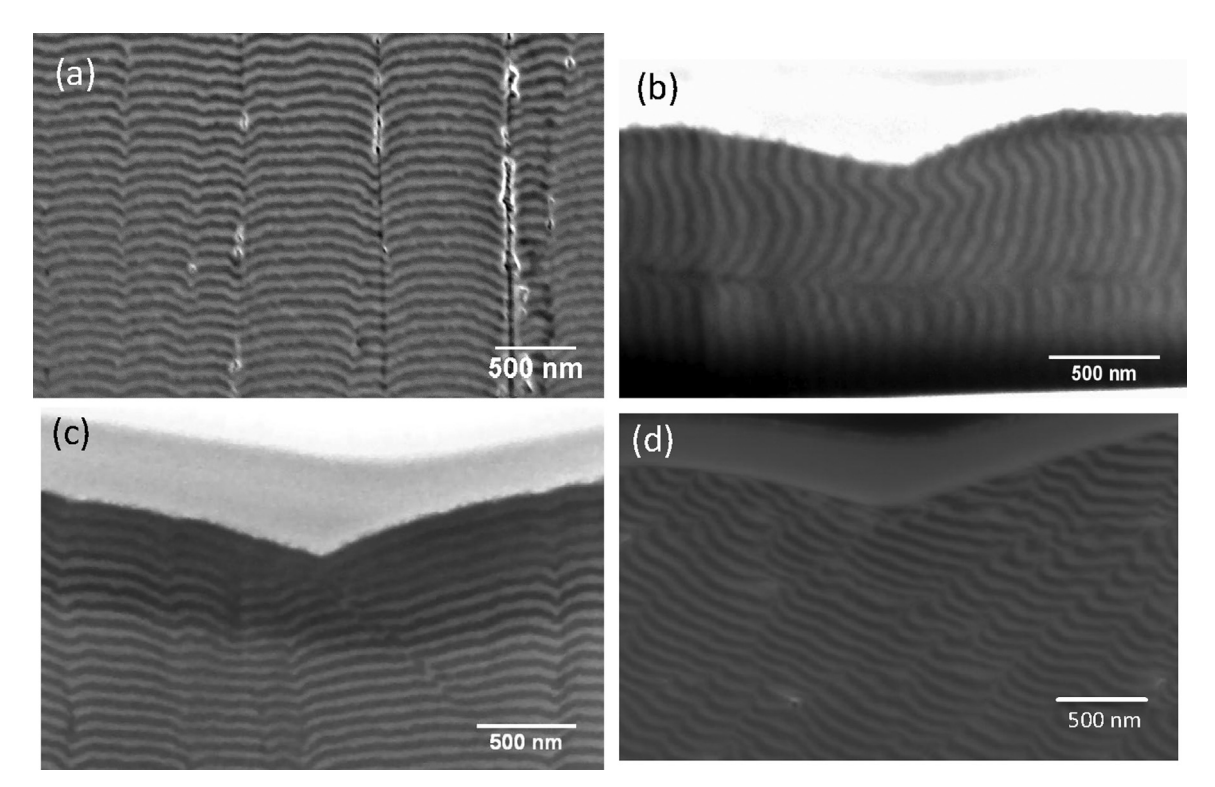


Fig. 1. SEM image of the undeformed nanolaminate microstructure (a) as well as the damaged regions underneath parallel (b), perpendicular (c), and inclined (d) indentations.

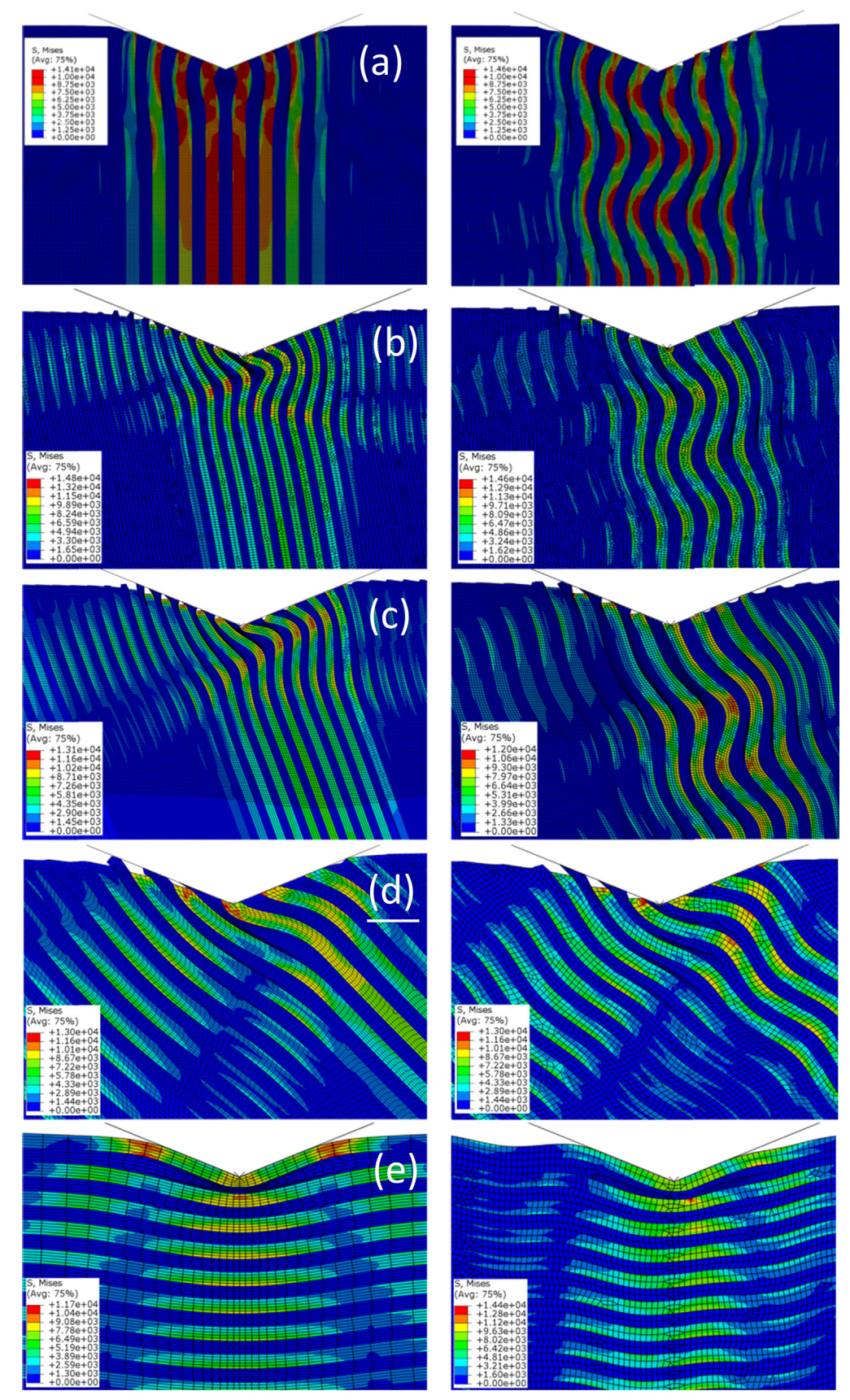


Fig. 2. FEM von Mises effective stress contours of parallel indentation of flat (left) and wavy (right) microstructures for loading at 0° , 10° , 20° , 45° , and 90° (a–e respectively). The wavy microstructure shows more pronounced buckling of the layers except for the 90° case which shows little difference in behavior.

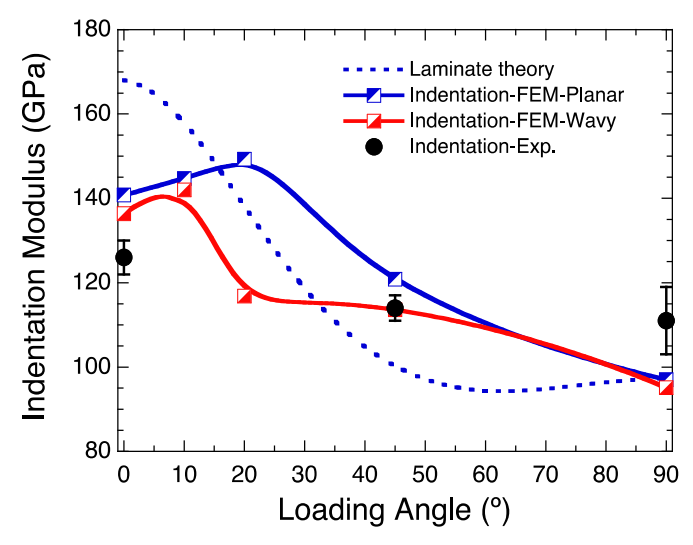


Fig. 3. Effect of loading angle on relative stiffness with respect to perpendicular loading (90°) . The solid lines are the predictions of laminate theory for uniaxial loading. The half full symbols represent the results of the FEM indentation simulations for planar and wavy layers and the full symbols correspond to the experimental results.

using the 2D plane strain model, an effective indentation modulus is calculated to approximate the true value. The effective indentation modulus was calculated through the following scaling law, obtained from dimensional analysis that:

$$S = \alpha \frac{E}{\left(1 - \nu^2\right)\sqrt{A}} \tag{1}$$

where S is the initial stiffness of the unloading portion of the simulated load–displacement curve, E and ν are the elastic constants of the material, A is the indentation contact area and α is the proportionality constant obtained through an axisymmetric FE simulation of the Al/SiC nanolaminate under perpendicular loading.

3. Results and discussion

Both the hardness and modulus values measured using nanoindentation show an increasing trend as the layers become more aligned with the loading axis, as shown in Table 1. Using laminate theory [10], the elastic modulus variation with loading direction should vary according to:

$$E = E_L \left[\cos^4 \theta + \frac{E_L}{E_T} \sin^2 \theta + \frac{1}{4} \left(\frac{E_L}{G_{LT}} - 2\nu_{LT} \right) \sin^2 2\theta \right]$$
 (2)

where θ is the loading angle, E_L is the longitudinal (isostrain) modulus, E_T is the transverse (isostress) modulus, G_{LT} is the inplane shear modulus obtained from the inverse rule of mixtures of the constituent layers and ν_{LT} is the in-plane Poisson's modulus, obtained from the rule of mixtures of the constituents. The theoretical perpendicular (isostress) and parallel (isostrain) moduli are also given in Table 1. In comparing the experimental and theoretical values, it is observed that the modulus is less dependent on orientation than the analytical solution, with the predicted isostrain modulus being significantly higher than the value measured using nanoindentation. This difference can be rationalized by the limitations inherent with indentation techniques as well as by the deviation from ideal flat layers in the material microstructure. Modeling helps shed light onto both of these concerns by simulating an indenter geometry as well as allowing for imperfections

in the microstructure.

As seen in the SEM image of the undeformed microstructure (Fig. 1(a)), the as-deposited layers show periodic waviness, which is an artifact of the columnar growth morphology followed by the Al layers [21]. This microstructural detail strongly affects the deformation behavior under loading conditions parallel and inclined to the layers. The waviness allows a buckling type of behavior to occur at much lower stresses than what would be expected for a perfectly flat structure because the preexisting undulations allow bending of the SiC layers to occur much more easily. This buckling behavior can be seen in the FIB cross section of the parallel (Fig. 1b) and inclined (Fig. 1d) indentations, in contrast to indentations in the perpendicular direction (Fig. 1c) which deform by plastic flow in the Al layers and localized shear bands.

This buckling behavior due to the layer waviness is also observed when modeling indentations in all orientations except the perpendicular case, as shown in Fig. 2. Indentation at inclined angles showed a combination of behaviors, with the right indenter face producing buckling behavior as in the parallel orientation and the left face causing plastic flow of the Al layers as in the perpendicular orientation. In addition to changing the morphology of the deformation, this buckling behavior has a large effect on the mechanical response of the multilayer. This change in behavior due to the layer geometry can qualitatively be seen by considering the SiC layers to be curved beams, where the apparent stiffness of these beams sharply decrease under axial loading with decreased radius [22]. As seen in Fig. 3, although the waviness decreases the stiffness of the material in all orientations, the largest effect is observed around 20° between the layers and the loading axis. The difference in the modeled modulus was shown to be up to 20 percent, highlighting that even small changes in the nanostructural details can have a significant impact on the resultant mechanical behavior.

It should also be noted that although traditional laminate theory predicts that the highest modulus would be observed in the parallel indentations, FEM of small angle inclinations yield higher moduli. This is caused by the indenter geometry. Since the faces of the indenter are angled, an inclination of $\sim 20^{\circ}$ will make the layers perpendicular to an indenter face, increasing the measured stiffness. In addition to this effect, the indenter geometry also affects the imposed stress state. In contrast to the rule of mixtures assumptions, the stress state underneath the indenter is neither uniaxial nor uniform. This causes the overall indentation response to have some contribution from both the parallel and perpendicular directions. Therefore, it is expected that the moduli measured using indentation would fall somewhere between the moduli which would be measured using bulk techniques, which is corroborated by the experimental and FEM results showing a weaker dependence on orientation than the moduli predicted by classical laminate theory.

4. Conclusions

In summary, a combination of experimental and FEM results have shown the following for Al–SiC nanolaminate composites:

- The anisotropic behavior of these materials was characterized for the first time. The modulus and hardness in the direction parallel to the layers was shown to be greater than in the perpendicular and inclined directions.
- Due to the multi-axial stress state beneath the indenter and the laminate waviness, indentation measurements do not show as large differences between orientations as seen in the calculations based on laminate theory.
- Layer waviness predisposes the SiC layers to buckling

- deformation when loaded in the parallel and inclined orientations, leading to a more compliant response compared to the flat microstructure.
- Layer curvature reduces the stiffness of the multilayer in all orientations but much more drastically in the parallel and inclined orientations, especially where the layers are perpendicular to the indenter faces (~20°).

The authors would like to acknowledge the National Science Foundation Materials World Network (contract DMR-1209928, Dr. Lynnette Madsen, Program Manager) and the Spanish Ministry of Economy (PCIN-2013-029) for financial support of this research as well as the LeRoy Erying Center for Solid State Science for the use of their microscopy facilities. The sample deposition was performed at the Center for Integrated Nanotechnologies, an Office of Science User Facility operated for the U.S. Department of Energy (DOE) Office of Science by Los Alamos National Laboratory (Contract DE-AC52-06NA25396) and Sandia National Laboratories (Contract DE-AC04-94AL85000). LWY acknowledges the China Research Council for his PhD scholarship.

References

- N. Chawla, D. Singh, Y.-L. Shen, G. Tang, K. Chawla, Indentation mechanics and fracture behavior of metal/ceramic nanolaminate composites, J. Mater. Sci. 43 (2008) 4383–4390.
- [2] N.A. Mara, D. Bhattacharyya, P. Dickerson, R.G. Hoagland, A. Misra, Deformability of ultrahigh strength 5nm cu-nb nanolayered composites, Appl. Phys. Lett. 92 (23) (2008) 1–3.
- [3] D. Singh, N. Chawla, Scratch resistance of al/sic metal/ceramic nanolaminates, J. Mater. Res. 27 (2012) 278–283.
- [4] W. Li, B. Kabius, O. Auciello, Science and technology of biocompatible thin films for implantable biomedical devices, Eng. Med. Biol. Soc. (EMBC), Annu. Int. Conf. IEEE (2010) 6237–6242.
- [5] G.S. Hickey, S.-S. Lih, T.W. Barbee Jr., Development of nanolaminate thin-shell mirrors, Proc. SPIE 4849 (2002) 63–76.
- [6] X. Deng, M. Koopman, N. Chawla, K. Chawla, Young's modulus of (cu, ag)-sn intermetallics measured by nanoindentation, Mater. Sci. Eng.: A 364 (2004)

- 240-243.
- [7] M. Dudek, N. Chawla, Nanoindentation of rare earth-sn intermetallics in pbfree solders, Intermetallics 18 (5) (2010) 1016–1020.
- [8] S. Lotfian, C. Mayer, N. Chawla, J. Llorca, A. Misra, J. Baldwin, J. Molina-Aldar-egua, Effect of layer thickness on the high temperature mechanical properties of Al/SiC nanolaminates, Thin Solid Films 571 (2) (2014) 260–267.
- [9] S.S. Singh, C. Schwartzstein, J.J. Williams, X. Xiao, F.D. Carlo, N. Chawla, 3d microstructural characterization and mechanical properties of constituent particles in al 7075 alloys using x-ray synchrotron tomography and nanoindentation, J. Alloy. Compd. 602 (2014) 163–174.
- [10] B. Agarwal, L. Broutman, Analysis and Performance of Fiber Composites, Ser. SPE Monographs, Wiley, Somerset, NI, 1990.
- [11] G. Tang, Y.-L. Shen, D. Singh, N. Chawla, Indentation behavior of metal-ceramic multilayers at the nanoscale: Numerical analysis and experimental verification, Acta Mater. 58 (6) (2010) 2033–2044.
- [12] D. Bhattacharyya, N. Mara, P. Dickerson, R. Hoagland, A. Misra, Compressive flow behavior of Al-Tin multilayers at nanometer scale layer thickness, Acta Mater. 59 (10) (2011) 3804–3816.
- [13] Y. Chen, Y. Liu, C. Sun, K. Yu, M. Song, H. Wang, X. Zhang, Microstructure and strengthening mechanisms in cu/fe multilayers, Acta Mater. 60 (18) (2012) 6312–6321.
- [14] R.D. Jamison, Y.-L. Shen, Indentation and overall compression behavior of multilayered thin-film composites: effect of undulating layer geometry, J. Compos. Mater. (2015).
- [15] S. Lotfian, M. Rodriguez, K. Yazzie, N. Chawla, J. Llorca, J. Molina-Aldareguia, High temperature micropillar compression of al/sic nanolaminates, Acta Mater. 61 (12) (2013) 4439–4451.
- [16] D. Singh, N. Chawla, G. Tang, Y.-L. Shen, Micropillar compression of al/sic nanolaminates, Acta Mater. 58 (20) (2010) 6628–6636.
- [17] N. Verma, V. Jayaram, Role of interface curvature on stress distribution under indentation for ZrN/Zr multilayer coating, Thin Solid Films 571 (2) (2014) 283–289 (multilayers 2013).
- [18] C. Mayer, N. Li, N. Mara, N. Chawla, Micromechanical and in situ shear testing of al-sic nanolaminate composites in a transmission electron microscope (tem), Mater. Sci. Eng.: A 621 (2015) 229–235.
- [19] X. Li, B. Bhushan, A review of nanoindentation continuous stiffness measurement technique and its applications, Mater. Charact. 48 (1) (2002) 11–36
- [20] G. Pharr, J. Strader, W. Oliver, Critical issues in making small-depth mechanical property measurements by nanoindentation with continuous stiffness measurement, J. Mater. Res. 24 (2009) 653–666.
- [21] D. Singh, N. Chawla, Y.-L. Shen, Focused ion beam (fib) tomography of nanoindentation damage in nanoscale metal/ceramic multilayers, Mater. Charact. 61 (4) (2010) 481–488.
- [22] C. Gonzalez, J. LLorca, Stiffness of a curved beam subjected to axial load and large displacements, Int. J. Solids Struct. 42 (2005) 1537–1545.